The focus-saddle boundary bifurcation in planar piecewise linear systems Application to the analysis of memristor oscillators

Enrique Ponce[a], Javier Ros[a], Elísabet Vela[b]

[a] *Departamento de Matemática Aplicada II, Escuela Técnica Superior de Ingeniería Universidad de Sevilla, Spain*
[b] *Departamento de Geometría y Topología, Facultad de Matemáticas Universidad de Sevilla, Spain*

Abstract

Among the boundary equilibrium bifurcations in planar continuous piecewise linear systems with two zones separated by a straight line, the focus-saddle bifurcation corresponds with a one-parameter transition from a situation without equilibria to a configuration with two equilibria, namely a focus and a saddle point. Depending on the dynamics of the two linear systems involved, the focus can appear surrounded by a limit cycle, by a saddle-loop (homoclinic connection) or by nothing else.

After introducing a criticality coefficient whose sign discriminates the different possible situations, the focus-saddle bifurcation is quantitatively characterized for the first time. The analysis requires to work in a more general framework, as is the family of planar refracting linear systems with two zones, for which a new result about existence and uniqueness of limit cycles and saddle-loops is also shown.

Email addresses: eponcem@us.es (Enrique Ponce), javieros@us.es (Javier Ros), elivela@us.es (Elísabet Vela)

The achieved results are applied to the study of oscillations in an electronic circuit involving a single memristor cell, showing rigorously the appearance of limit cycles via the focus-saddle bifurcation analyzed in the paper.

Keywords: Qualitative Theory of ODEs, Piecewise linear systems, limit cycles, bifurcations

---

1. Introduction and statement of main results

In this paper, we consider continuous piecewise linear differential systems (PWL systems, for short) with two linearity zones separated by a straight line representing the only non-smoothness manifold in the phase plane. Such systems are relevant in different application fields and have been studied by several authors; see [1, 2] and references therein for a thorough introduction and a revision of the state of the art in the study of these systems.

Our main goal is to characterize in a precise way the focus-saddle boundary equilibrium bifurcation for such continuous PWL systems, a phenomenon leading to the creation/annihilation of two equilibrium points (a focus and a saddle) along with the possible appearance of a limit cycle or a saddle connection surrounding the focus, see Chapter 5 of [1] and [3, 4].

We will assume without loss of generality that the linearity regions in the phase plane are the left and right half-planes,

$$S_L = \{(x, y) \in \mathbb{R}^2 : x < 0\}, \quad S_R = \{(x, y) \in \mathbb{R}^2 : x > 0\},$$

separated by the straight line $\Sigma = \{(x, y) \in \mathbb{R}^2 : x = 0\}$.

We proceed by considering a specific family of systems within the more

general setting of discontinuous systems. Namely, we first study discontinuous PWL systems for which the two involved linear vector fields share their normal component to Σ at all the points of such discontinuity manifold. These systems are known as *refracting systems* and are characterized by not having any sliding segment in the discontinuity manifold Σ, see [5]. In other words, orbits arriving at Σ can be naturally extended by concatenating solutions from both sides, since all the orbits hit Σ in the so-called *sewing* or crossing points, see [6]. In fact, refracting systems belong to the slightly wider class of *sewing systems*, characterized by sharing only the sign of the normal component to the discontinuity manifold Σ, see [7].

To reduce the number of parameters in the analysis, we start by introducing a canonical form for Σ-refracting PWL systems. A general discontinuous PWL system can be written as

$$\dot{\mathbf{x}} = \begin{cases} A_R\mathbf{x} + \mathbf{b}_R, & \text{if } x \in S_R, \\ A_L\mathbf{x} + \mathbf{b}_L, & \text{if } x \in S_L \cup \Sigma, \end{cases} \tag{1}$$

where $\mathbf{x} = (x, y) \in \mathbb{R}^2$ is the vector of state variables, $A_R = (a_{ij}^R)$ and $A_L = (a_{ij}^L)$ are 2×2 constant matrices, $\mathbf{b}_R = (b_1^R, b_2^R)^T$, $\mathbf{b}_L = (b_1^L, b_2^L)^T \in \mathbb{R}^2$ are constant vectors, and the point denotes derivatives with respect to the time variable s. Imposing now the refracting condition on these systems, we require that for all $\mathbf{x} = (0, y)^T \in \Sigma$, with $y \in \mathbb{R}$,

$$\mathbf{e}_1^T \left(A_R\mathbf{x} + \mathbf{b}_R\right) = \mathbf{e}_1^T \left(A_L\mathbf{x} + \mathbf{b}_L\right), \tag{2}$$

where $\mathbf{e}_1^T$ stands for the first unitary vector in row form. From (2) and some

elementary algebra, we must assume $a_{12}^L = a_{12}^R$ and $b_1^L = b_1^R$, so that systems to be studied become

$$\begin{aligned} \dot{\mathbf{x}} &= \begin{pmatrix} a_{11}^L & a_{12} \\ a_{21}^L & a_{22}^L \end{pmatrix} \mathbf{x} + \begin{pmatrix} b_1 \\ b_2^L \end{pmatrix} \text{ if } \mathbf{x} \in S_L \cup \Sigma, \\ \dot{\mathbf{x}} &= \begin{pmatrix} a_{11}^R & a_{12} \\ a_{21}^R & a_{22}^R \end{pmatrix} \mathbf{x} + \begin{pmatrix} b_1 \\ b_2^R \end{pmatrix} \text{ if } \mathbf{x} \in S_R, \end{aligned} \tag{3}$$

where $a_{12} = a_{12}^L = a_{12}^R$ and $b_1 = b_1^L = b_1^R$.

Remark 1. Note that it is natural to assume $a_{12} \neq 0$ in (3) if one wants to cope with non-elementary dynamics. Otherwise, we should have $\dot{x} = b_1$ for all the points in Σ, so that all the orbits would cross Σ in the same direction. Furthermore, the dynamics of the first variable would be decoupled from the second one in the whole plane, oscillations would be not possible and the system could not exhibit a proper two-dimensional dynamics.

As done in Proposition 3.1 of [8], by assuming $a_{12} \neq 0$ and applying the homeomorphism $\widetilde{\mathbf{x}} = h(\mathbf{x})$ given by

$$\widetilde{\mathbf{x}} = \begin{pmatrix} 1 & 0 \\ a_{22}^L & -a_{12} \end{pmatrix} \mathbf{x} - \begin{pmatrix} 0 \\ b_1 \end{pmatrix} \text{ if } \mathbf{x} \in S_L \cup \Sigma,$$

$$\widetilde{\mathbf{x}} = \begin{pmatrix} 1 & 0 \\ a_{22}^R & -a_{12} \end{pmatrix} \mathbf{x} - \begin{pmatrix} 0 \\ b_1 \end{pmatrix} \text{ if } \mathbf{x} \in S_R,$$

after dropping tildes, we transform systems (3) into the following discontin-

uous Liénard canonical form for refracting systems

$$\begin{aligned}\dot{\mathbf{x}} &= \begin{pmatrix} t_L & -1 \\ d_L & 0 \end{pmatrix}\mathbf{x} - \begin{pmatrix} 0 \\ \mu_L \end{pmatrix} \text{ if } \mathbf{x} \in S_L \cup \Sigma, \\ \dot{\mathbf{x}} &= \begin{pmatrix} t_R & -1 \\ d_R & 0 \end{pmatrix}\mathbf{x} - \begin{pmatrix} 0 \\ \mu_R \end{pmatrix} \text{ if } \mathbf{x} \in S_R, \end{aligned} \tag{4}$$

where $\mu_L = a_{12}b_2^L - a_{22}^L b_1$, $\mu_R = a_{12}b_2^R - a_{22}^R b_1$, and $t_{\{L,R\}} = \operatorname{tr} A_{\{L,R\}}$, $d_{\{L,R\}} = \det A_{\{L,R\}}$ denote the traces and determinants of L- and R-matrices.

Remark 2. It should be noticed that if we start from a continuous PWL vector field in (1) instead of a refracting system, then the continuity requirement at Σ provides the conditions $a_{22}^L = a_{22}^R$ and $b_2^L = b_2^R$. Thus, in such a case we obtain $\mu_L = \mu_R$, and the above canonical form turns out to be continuous.

Regarding the canonical form for refracting systems (4), it is evident that our systems constitute a specific case of Filippov systems in which, excepting the origin, all the points in Σ belong to the so-called crossing or sewing set, not having a proper sliding set. The origin can be thought as a tangency point or a singular isolated sliding point, see [6]. When one or both of the two vector fields vanishes at the origin, such a point is a boundary equilibrium point; otherwise we can have a pseudo-equilibrium point or even a regular point, see [9].

Remark 3. The Liénard canonical form for refracting systems (4) is invari-

ant under the following transformations:

$$\Pi_1 : (s, x, y, t_L, t_R, \mu_L, \mu_R, d_L, d_R) \longmapsto (-s, -x, y, -t_R, -t_L, -\mu_R, -\mu_L, d_R, d_L)$$
$$\Pi_2 : (s, x, y, t_L, t_R, \mu_L, \mu_R, d_L, d_R) \longmapsto (-s, x, -y, -t_L, -t_R, \mu_L, \mu_R, d_L, d_R)$$
$$\Pi_3 : (s, x, y, t_L, t_R, \mu_L, \mu_R, d_L, d_R) \longmapsto (s, -x, -y, t_R, t_L, -\mu_R, -\mu_L, d_R, d_L)$$

Note that as a result of transformation Π_1, we should obtain the symmetrical version of the system with respect to the y-axis along with a reversal of time that maintains the rotation sense of orbits around the origin. Similarly, the transformation Π_2 returns the symmetrical version of the system with respect to the x-axis, while $\Pi_3 = \Pi_1 \circ \Pi_2 = \Pi_2 \circ \Pi_1$ gets the mirror image of the system respect to the origin of coordinates.

In canonical form (4), the parameter pair (μ_L, μ_R) controls the number and position of the equilibrium points. From (4) and assuming $d_L d_R \neq 0$, the candidates to be equilibrium points in the left and right zones are respectively

$$\bar{\mathbf{x}}_L = \left(\frac{\mu_L}{d_L}, t_L \frac{\mu_L}{d_L}\right) \text{ and } \bar{\mathbf{x}}_R = \left(\frac{\mu_R}{d_R}, t_R \frac{\mu_R}{d_R}\right).$$

Obviously, apart from the boundary cases, $\bar{\mathbf{x}}_L$ is a real equilibrium only if $\mu_L d_L < 0$, and so is $\bar{\mathbf{x}}_R$ if $\mu_R d_R > 0$. Otherwise, one can speak of virtual equilibrium points, since they would not be in the corresponding zone.

Boundary equilibrium bifurcations in the case of determinants with equal sign were studied in [10]. Here, we consider the case of determinants with different sign, and for definiteness we will pay attention to the configuration

$$d_L > 0,\ d_R < 0, \text{ and either } \mu_L \mu_R > 0 \text{ or } \mu_L = \mu_R = 0, \tag{5}$$

which has obvious dual cases that could be analyzed via Remark 3. In this situation, regarding equilibria of systems (4), we have the following general result. The proof is direct and is omitted.

Proposition 1 *For refracting systems* (4) *fulfilling hypotheses* (5) *the following statements hold.*

a) If $\mu_L = \mu_R = 0$, then the origin is the single equilibrium point.

b) If $\mu_L \mu_R > 0$, then the following cases arise.

(i) If $\mu_L < 0$ or equivalently $\mu_R < 0$, then the system has two equilibrium points, a saddle point in the right zone and an anti-saddle point (to be a node or a focus) in the left zone.

(ii) If $\mu_L > 0$ or equivalently $\mu_R > 0$, then the system has no equilibrium points.

It is easy to rule out the existence of periodic orbits in all the cases where there are no equilibrium points of focus type, that is, when the two dynamics involved are of type node and saddle. Therefore, from the dynamical point of view, the most interesting case under hypotheses (5) is the focus-saddle configuration, the case to be considered in what follows. When the left dynamics is of focus type, having then a saddle dynamics in the right half plane, it is also clear that in the cases of statement (a) and $(b.ii)$ there cannot be limit cycles. Effectively, every limit cycle must use the two half planes, and then it is not possible to define any return map on the y-axis by using the orbits in the right part.

Regarding the possible existence of a saddle connection or limit cycles in the focus case of statement $(b.i)$ of Proposition 1, a first useful result is

the following. From Proposition 3.7 in [8], which is a direct consequence of Bendixson's criterion, we know that the inequality $t_L t_R < 0$ is a necessary condition for that; for definiteness, we take $t_L > 0$ and $t_R < 0$.

Proposition 2 *Considering refracting systems* (4) *under hypotheses* $4d_L - t_L^2 > 0$ *and* $d_R < 0$ *with* $t_L > 0$, $t_R < 0$, $\mu_L < 0$, $\mu_R < 0$, *if there exists a periodic orbit then it is a unique stable limit cycle and there are no homoclinic connections. Furthermore, if there exists a homoclinic connection then it is stable as seen from its interior and there are no periodic orbits.*

Proposition 2 will be shown in Section 3. Note that, within the realm of sewing planar piecewise linear systems, Proposition 2 gives a uniqueness statement both for limit cycles and saddle-loops in the focus-saddle case that cannot be obtained from the recent analysis made in [7]. Effectively, the condition $\mu_L < 0$ implies that we have a real focus and so a visible tangency for orbits approaching the origin from the left. Therefore, the origin is not a Σ-*monodromic singularity* in the terminology of the quoted paper. Thus, Proposition 2 represents a new uniqueness result that was lacking for a complete analysis of sewing linear systems in the focus-saddle configuration.

Next result characterizes completely the existence of closed orbits in systems (4) in the focus-saddle configuration. The main ideas behind the techniques are similar to the ones needed to show Theorem 2.b.3 in [11], but here we must extend them to cope with the family of refracting systems. Furthermore, the discontinuous character of such a family required specific new uniqueness results for closed orbits, as given in Proposition 2 above. We introduce some auxiliary parameters to be crucial in the rest of the paper,

namely

$$\omega_L = \frac{\sqrt{4d_L - t_L^2}}{2}, \quad \gamma_L = \frac{t_L}{2\omega_L}, \quad \omega_R = \frac{\sqrt{t_R^2 - 4d_R}}{2}, \quad \gamma_R = \frac{t_R}{2\omega_R}, \tag{6}$$

and

$$\rho = \frac{\mu_R}{\mu_L} \cdot \frac{\omega_L(1+\gamma_L^2)}{\omega_R(1-\gamma_R^2)}, \tag{7}$$

along with the angles

$$\theta_\pm = \pm 2 \arctan\left(\sqrt{1 + \left[\gamma_L + \rho(\gamma_R \pm 1)\right]^2} \mp \left[\gamma_L + \rho(\gamma_R \pm 1)\right]\right). \tag{8}$$

Note that from the condition $d_R < 0$ we have $\gamma_R \in (-1, 1)$ and so $\rho > 0$ when $\mu_L < 0$, $\mu_R < 0$. We can state the following result.

Theorem 1 *Consider refracting systems* (4) *under hypotheses* $4d_L - t_L^2 > 0$ *and* $d_R < 0$ *with* $t_L > 0$, $t_R < 0$, $\mu_L < 0$, $\mu_R < 0$, *and* γ_L, γ_R, ρ, *and* $\theta_\pm$ *as defined in* (6)-(8). *If we define the values*

$$V_\pm = \pm e^{\gamma_L \theta_\pm} \sqrt{1 + \left[\gamma_L + \rho(\gamma_R \pm 1)\right]^2}, \tag{9}$$

then the following statements hold.

a) If $e^{\pi\gamma_L} V_+ + V_- < 0$, *then the unstable focus is surrounded by one stable limit cycle.*

b) If $e^{\pi\gamma_L} V_+ + V_- = 0$, *then the unstable focus is surrounded by an homoclinic orbit and there are no limit cycles.*

c) If $e^{\pi\gamma_L} V_+ + V_- > 0$, *then the system does not have either limit cycles*

or homoclinic connections.

Theorem 1 is shown in Section 3.

When we consider the case $\mu_L = \mu_R = \mu$ in systems (4), we are dealing with a continuous system, namely

$$\begin{aligned} \dot{\mathbf{x}} &= \begin{pmatrix} t_L & -1 \\ d_L & 0 \end{pmatrix} \mathbf{x} - \begin{pmatrix} 0 \\ \mu \end{pmatrix} \text{ if } \mathbf{x} \in S_L \cup \Sigma, \\ \dot{\mathbf{x}} &= \begin{pmatrix} t_R & -1 \\ d_R & 0 \end{pmatrix} \mathbf{x} - \begin{pmatrix} 0 \\ \mu \end{pmatrix} \text{ if } \mathbf{x} \in S_R, \end{aligned} \tag{10}$$

where we take the parameter μ as the only bifurcation parameter.

From Proposition 1 and assuming hypotheses (5) with $\mu = \mu_R = \mu_L$, we first note that for $\mu < 0$ we have a situation with two equilibrium points (a focus or a node plus a saddle); these two points collide in a single equilibrium point for $\mu = 0$ and disappear, both becoming virtual equilibrium points for $\mu > 0$. In this last case $\mu > 0$, it is easy to see that the system dynamics excludes equilibrium points and periodic orbits, see Fig. 1. For $\mu < 0$ we can also rule out the existence of periodic orbits and saddle-loops (homoclinic connections) in the node-saddle case; from Theorem (1) both types of closed orbits are possible however in the focus-saddle case, see also [12, 13].

In the previous work [10], boundary equilibrium bifurcations were considered for such PWL systems in the so called *persistence* scenario, characterized by the condition $d_L d_R > 0$. Under this condition, by moving the parameter μ from negative to positive values or vice versa, a transition of the unique equilibrium point through the boundary manifold between linearity zones is

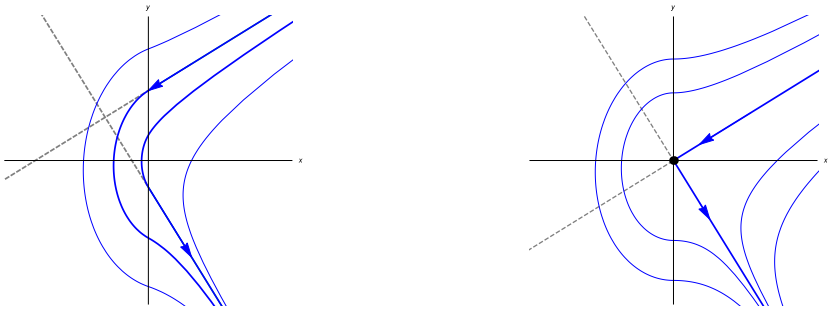

Figure 1: The case $\mu > 0$ and the critical situation $\mu = 0$.

guaranteed, being possible the simultaneous generation of limit cycles.

Here, we deal instead with boundary equilibrium bifurcations in the *non-smooth fold* scenario, since by moving the parameter μ two different branches of equilibria collide in the boundary to disappear in the other side of the bifurcation. We study now the focus-saddle boundary equilibrium bifurcation for PWL systems (10), regarding the simultaneous generation of a limit cycle, a saddle loop or nothing else, depending on the dynamics properties of the two involved vector fields. It is our main goal to characterize quantitatively which one of the above three alternatives actually appears: a problem that, up to the best of our knowledge had not been solved before and turns out to be a necessary first step to study the same bifurcation in more general non-PWL frameworks, as done in [14] for the Andronov-Hopf bifurcation.

Our second main contribution comes to fill a gap in the bifurcation theory of continuous PWL systems. Indeed, the focus-saddle bifurcation already appeared in the celebrated book [1], but there was a lack of quantitative characterization, see Theorem 5.2.2.b.ii in the quoted work. We use again the auxiliary parameters introduced in (6)-(8), but note that here the parameter

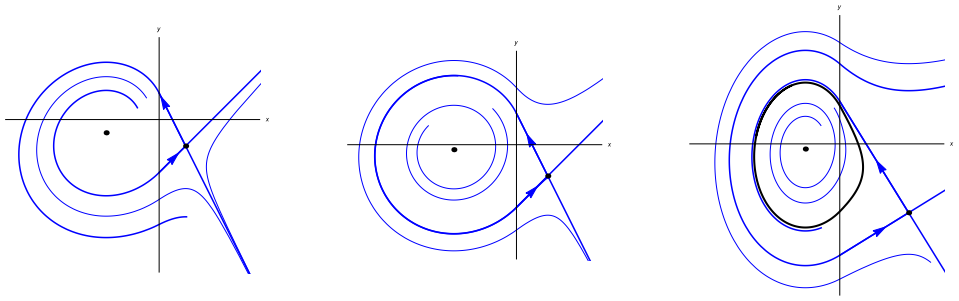

Figure 2: From left to right, the three possibilities when $\mu < 0$ for the focus-saddle bifurcation: $\delta > 0$, $\delta = 0$, and $\delta < 0$.

ρ reduces to

$$\rho = \frac{\omega_L(1+\gamma_L^2)}{\omega_R(1-\gamma_R^2)}. \tag{11}$$

Theorem 2 *Consider continuous PWL systems* (10) *with* $t_L > 0$, $t_R < 0$, *under the hypotheses of left focus dynamics* $4d_L - t_L^2 > 0$, *and right saddle dynamics* $d_R < 0$, *so that* γ_L, γ_R *are given in* (6), ρ *as in* (11) *and* $\theta_\pm$ *as in* (8). *Define the criticality coefficient* δ *as follows,*

$$\delta = e^{2\gamma_L(\pi+\theta_+-\theta_-)} - \frac{1+[\gamma_L+\rho(\gamma_R-1)]^2}{1+[\gamma_L+\rho(\gamma_R+1)]^2}. \tag{12}$$

Regarding μ *as the only bifurcation parameter, the system undergoes a saddle-focus boundary equilibrium bifurcation for* $\mu = 0$*; that is, we pass from a situation without equilibria for* $\mu > 0$ *to a single boundary equilibrium at* $\mu = 0$, *and to a configuration with an unstable focus and a saddle for* $\mu < 0$. *Furthermore, the following statements hold.*

a) If $\delta < 0$ *the boundary equilibrium bifurcation leads also for* $\mu < 0$ *to one stable limit cycle surrounding the unstable focus and no homoclinic connections. The size of the limit cycle evolves linearly with* $|\mu|$.

b) If $\delta = 0$ the boundary equilibrium bifurcation leads also for $\mu < 0$ to a homoclinic connection (saddle-loop) surrounding the unstable focus and no limit cycles. The size of the saddle-loop evolves linearly with $|\mu|$.

c) If $\delta > 0$ then the boundary equilibrium bifurcation arising for $\mu = 0$ does not involve any limit cycle or homoclinic connection.

The proof of Theorem 2 is given in Section 3. See Fig. 1 and 2 for the different configurations mentioned in above statements.

Example 1. To illustrate the above result, we consider a concrete model in the form (10), namely

$$\dot{\mathbf{x}} = \begin{pmatrix} 1/2 & -1 \\ 5 & 0 \end{pmatrix} \mathbf{x} - \begin{pmatrix} 0 \\ \mu \end{pmatrix} \text{ if } \mathbf{x} \in S_L \cup \Sigma,$$

$$\dot{\mathbf{x}} = \begin{pmatrix} -1 & -1 \\ -1 & 0 \end{pmatrix} \mathbf{x} - \begin{pmatrix} 0 \\ \mu \end{pmatrix} \text{ if } \mathbf{x} \in S_R,$$

which is equivalent to Example 5.5 in p. 228–229 of [1], but note that our parameter μ is the opposite to the one appearing in the quoted book.

From (6), computations give $\omega_L = \sqrt{79}/4$, $\gamma_L = 1/\sqrt{79}$, $\omega_R = \sqrt{5}/2$, $\gamma_R = -\sqrt{5}/2$, while from (11) we get $\rho = 10\sqrt{5}/\sqrt{79}$. Then, from (8) we obtain $\theta_\pm = \pm 2 \arctan\left(\left(\left(2\sqrt{165 \mp 45\sqrt{5}} \pm 9 - 10\sqrt{5}\right)/\sqrt{79}\right)\right.$. After some simplifications, we finally obtain

$$\delta = \exp\left(\frac{2\pi + 4\arctan\left(\frac{6\sqrt{19}-17}{\sqrt{395}}\right)}{\sqrt{79}}\right) - \frac{1}{38}\left(83 + 33\sqrt{5}\right) \approx -1.66363,$$

so that Theorem 2 assures that for $\mu < 0$ we have a stable limit cycle surrounding the unstable focus. Thus, the qualitative statement given in Theorem 5.2.2.b.ii of [1] is substituted by a rigorous quantitative assertion, coming from Theorem 2.

It is worth to emphasize the rather involved expression for the criticality coefficient δ. This feature arises because of the lack of smoothness in PWL systems, which precludes any local analysis; in fact, the semi-homogeneity property of systems (10) with respect to the parameter μ, explains why it is possible to characterize the bifurcation only after a global analysis.

The applicability of Theorem 2 is greater than it seems. In fact, we could state evident dual versions of this theorem for other three different cases: (i) $t_L < 0$, $t_R > 0$ keeping $4d_L - t_L^2 > 0$ and $d_R < 0$; (ii) $t_L > 0$, $t_R < 0$ but assuming $d_L < 0$ and $4d_R - t_R^2 > 0$; and (iii) $t_L < 0$, $t_R > 0$ with $d_L < 0$ and $4d_R - t_R^2 > 0$; all these cases can be dealt with by resorting to Remark 3 and will not be explicitly listed.

Remark 4. It is interesting to note that if we let $\gamma_L \to 0$ (which corresponds to let $t_L \to 0$ keeping $d_L > 0$ constant so that $\omega_L \to \sqrt{d_L}$) then we have that the limit value δ_* for δ is

$$\delta_* = \lim_{\gamma_L \to 0} \delta = 1 - \frac{1 + \rho_*^2(\gamma_R - 1)^2}{1 + \rho_*^2(\gamma_R + 1)^2} = \frac{4\rho_*^2 \gamma_R}{1 + \rho_*^2(\gamma_R + 1)^2} < 0,$$

where

$$\rho_* = \lim_{\gamma_L \to 0} \rho = \frac{\sqrt{d_L}}{\omega_R(1 - \gamma_R^2)}.$$

This negative limit value δ_* indicates that whenever $\gamma_L > 0$ is sufficiently small, then $\delta < 0$ and the unstable focus is surrounded by one stable limit

cycle for $\mu < 0$. On the other hand, if $\gamma_L = 0$ and $\mu < 0$ then we have a bounded linear center whose outermost closed orbit is tangent to Σ from the left. Then, if we start from $\gamma_L = 0$, any small increase in γ_L leads to a limit cycle bifurcating from the center, a phenomenon that has been qualitatively and quantitatively studied in [13].

We want to emphasize that the bifurcation characterized in Theorem 2 has no counterpart within the realm of smooth vector fields. Effectively, we know that when a smooth system undergoes a bifurcation leading to the generation of two equilibrium points, the generic configuration corresponds with a saddle-node bifurcation. Thus, the saddle-focus situation studied here is specific to the class of piecewise linear systems.

As a final remark, Theorem 2 could be extended to the more general case of continuous piecewise smooth systems (not necessarily PWL systems), in the same spirit of the study made in [14] for the Andronov-Hopf bifurcation. Such extension should require to take into account the nonlinear terms in each vector field and is beyond the scope of this paper.

The rest of the paper is organized as follows. We show an interesting application of Theorem 2 to nonlinear electronics in Section 2, by considering a circuit already studied in [15] but allowing non-zero initial conditions, which is a fact of special relevance to cope with the dynamical richness of these devices, see [16]. Some auxiliary results and the proofs of main results appear in Section 3.

2. Application to the analysis of memristor oscillators

We consider here an electronic circuit already analyzed in [15] and [11] under different hypotheses. For the sake of completeness, we include the derivation of the model, which is very similar to the one appeared in [11], but with an important novelty related to the consideration of non-zero initial conditions.

Following [15] memristors are two-terminal electronic passive devices for which a nonlinear relationship links charge and flux [17]. They are at the basis of future generation dynamic memories; as another important feature, nanoscale memristors have potential to reproduce the behavior of biological synapses. Here we apply our previous results to the analysis of an elementary oscillator endowed with one flux-controlled memristor, see Figure 3 and [18].

Note that in the shown circuit the values of L and C for the impedance and capacitance are positive constants, while the resistor has a negative value $-R$. We write from Kirchoff's laws

$$\begin{aligned} i_R(\tau) - i_L(\tau) = 0, \quad i_L(\tau) - i_C(\tau) - i_M(\tau) = 0, \\ v_C(\tau) - v_M(\tau) = 0, \quad v_R(\tau) + v_L(\tau) + v_C(\tau) = 0, \end{aligned}$$

where v, i stand for the voltage and current, respectively, across the corresponding element of the circuit. Next, we integrate with respect to time the above equations, and it should be emphasized that we do not assume zero

initial conditions as in [15], to get

$$\begin{aligned} q_R(\tau) - q_L(\tau) &= Q_1 = q_R(0) - q_L(0), && (13)\\ q_L(\tau) - q_C(\tau) - q_M(\tau) &= Q_2 = q_L(0) - q_C(0) - q_M(0), && (14)\\ \varphi_R(\tau) + \varphi_L(\tau) + \varphi_C(\tau) &= \Phi_1 = \varphi_R(0) + \varphi_L(0) + \varphi_C(0), && (15)\\ \varphi_C(\tau) - \varphi_M(\tau) &= \Phi_2 = \varphi_C(0) - \varphi_M(0), && (16) \end{aligned}$$

where q and φ stand respectively for the charge and flux associated to each element. The flux-charge characteristics of the memristor f_M is assumed as in [18] and [15] to be the symmetric piecewise linear function

$$f_M(x) = \begin{cases} b(x+1) - a & \text{for } x \leq -1,\\ ax & \text{for } -1 \leq x \leq 1,\\ b(x-1) + a & \text{for } x \geq 1, \end{cases}$$

where it is considered a passive memristor, and in particular $0 < a < b$. After recalling the constitutive equations of the bipoles, namely

$$\begin{aligned} \varphi_R(\tau) = -Rq_R(\tau), \quad \varphi_L(\tau) = L\frac{d}{d\tau}q_L(\tau),\\ q_C(\tau) = C\frac{d}{d\tau}\varphi_C(\tau), \quad q_M(\tau) = f_M(\varphi_M(\tau)), \end{aligned}$$

we arrive at the equations

$$\begin{aligned} \frac{d}{d\tau}\varphi_C(\tau) &= \frac{1}{C}q_C(\tau) = \frac{1}{C}\left[q_L(\tau) - q_M(\tau) - Q_2\right],\\ \frac{d}{d\tau}q_L(\tau) &= \frac{1}{L}\varphi_L(\tau) = \frac{1}{L}\left[-\varphi_C(\tau) - \varphi_R(\tau) + \Phi_1\right]. \end{aligned}$$

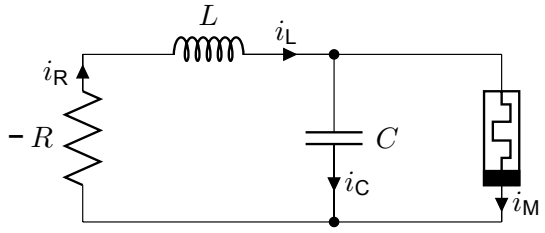

Figure 3: The simple oscillator with one memristor analyzed in this section. Note that the negative value $-R$ considered for the resistor makes it the only active element in the circuit.

We denote the state variables by $x_1 = \varphi_C(\tau)$ and $x_2 = q_L(\tau)$, and using (13) and (16), to write $\varphi_R(\tau) = -Rq_R(\tau) = -R(q_L(\tau) + Q_1)$ along with $q_M(\tau) = f_M(\varphi_M(\tau)) = f_M(\varphi_C(\tau) - \Phi_2)$, we have the differential system

$$\frac{dx_1}{d\tau} = \frac{1}{C}\left[-f_M(x_1 - \Phi_2) + x_2 - Q_2\right], \tag{17}$$

$$\frac{dx_2}{d\tau} = \frac{1}{L}\left[-x_1 + R(x_2 + Q_1) + \Phi_1\right]. \tag{18}$$

It turns out more convenient to translate variables by introducing $x = x_1 - \Phi_2$, and $y = x_2 - Q_2$, and write

$$\frac{dx}{d\tau} = \frac{1}{C}\left[-f_M(x) + y\right], \tag{19}$$

$$\frac{dy}{d\tau} = \frac{1}{L}\left[-x + R\tilde{y} + RQ_1 + RQ_2 + \Phi_1 - \Phi_2\right]. \tag{20}$$

As a consequence of the conservation laws of flux and charge, we can introduce the constant

$$h = RQ_1 + RQ_2 + \Phi_1 - \Phi_2 = \varphi_L(0) + \varphi_M(0) - R(q_C(0) + q_M(0)),$$

and using the parameters $\alpha = 1/C$, $\beta = R/L$, $\xi = 1/L$, we get the piecewise linear system

$$\frac{dx}{d\tau} = \alpha\left[-f_M(x) + y\right], \tag{21}$$

$$\frac{dy}{d\tau} = -\xi x + \beta y + \xi h. \tag{22}$$

We note that until here we have reproduced exactly the model achieved in [15], but with the additional constant term involving the parameter h, because here the initial conditions are not assumed to be zero. This fact, which introduces some lack of symmetry in the model, is of special relevance in the analysis of the dynamical richness of these oscillators, as remarked in [16]. Also, it should be noticed that we are dealing with a PWL system with three linearity regions, but as long as the interesting dynamics involves only two adjacent regions, we can take advantage of the results of Section 1.

To simplify the analysis, we rescale the time by taking as new time $\hat{\tau} = \alpha\tau$ and introduce the rescaled parameters $\tilde{h} = \xi h/\alpha$, $\tilde{\beta} = \beta/\alpha = RC/L > 0$, and $\tilde{\xi} = \xi/\alpha = C/L > 0$, to get

$$\frac{dx}{d\hat{\tau}} = -f_M(x) + y, \tag{23}$$

$$\frac{dy}{d\hat{\tau}} = -\tilde{\xi}x + \tilde{\beta}y + \tilde{h}. \tag{24}$$

In what follows we assume the same dynamical configuration analyzed in [15], namely saddle dynamics in the external zones and anti-saddle dynamics in the central zone, what leads to the condition $a\tilde{\beta} < \tilde{\xi} < b\tilde{\beta}$. Of course, we also assume the necessary condition for oscillation coming from Bendixson's

criterion, which amounts to have non-constant sign for the divergence of the vector field, that is, by computing traces, $a < \tilde{\beta} < b$.

It is straightforward to determine the number of equilibrium points and its topological type depending on the value of parameter $\tilde{h}$. Effectively, if we introduce the modified slope parameters $\tilde{a} = \tilde{\xi} - \tilde{\beta}a > 0$ and $\tilde{b} = \tilde{\xi} - \tilde{\beta}b < 0$, then the conditions for equilibria allow to eliminate the value of y, to get the equivalent condition $\tilde{h} = \tilde{f}(x) = \tilde{\xi}x - \tilde{\beta}f_M(x)$, where

$$\tilde{f}(x) = \begin{cases} \tilde{b}(x+1) - \tilde{a} & \text{for } x \leq -1, \\ \tilde{a}x & \text{for } -1 \leq x \leq 1, \\ \tilde{b}(x-1) + \tilde{a} & \text{for } x \geq 1. \end{cases}$$

The following result is now direct.

Proposition 3 *Considering system* (23)-(24) *under hypotheses* $0 < a < b$ *and* $a\tilde{\beta} < \tilde{\xi} < b\tilde{\beta}$*, the following statements hold.*

a) If $\tilde{h} < -\tilde{a}$ *or* $\tilde{h} > \tilde{a}$*, then there exists only one equilibrium point, which is a saddle located at*

$$\begin{cases} x = 1 + \dfrac{\tilde{h} - \tilde{a}}{\tilde{b}} > 1, \\ y = a + b\dfrac{\tilde{h} - \tilde{a}}{\tilde{b}}, \end{cases} \qquad \begin{cases} x = \dfrac{\tilde{h} + \tilde{a}}{\tilde{b}} - 1 < -1, \\ y = b\dfrac{\tilde{h} + \tilde{a}}{\tilde{b}} - a, \end{cases}$$

respectively.

b) If $|\tilde{h}| < \tilde{a}$*, then there exist three equilibrium points; one in the central zone located at*

$$x = \frac{\tilde{h}}{\tilde{a}}, \quad y = \frac{a\tilde{h}}{\tilde{a}},$$

which is of anti-saddle type, while the other two are saddles and located at the external zones, with the same coordinates given in statement (a).

c) When $|\tilde{h}| = \tilde{a}$, there appears a boundary equilibrium bifurcation giving rise to the generation or annihilation of two equilibria, namely a saddle and an anti-saddle.

Regarding Proposition 3, if we impose the condition of focus dynamics in the central zone, then we see that for both $\tilde{h} = -\tilde{a}$ and $\tilde{h} = \tilde{a}$ we have the focus-saddle bifurcation studied in this paper. Such a central focus configuration requires $(-a + \tilde{\beta})^2 < 4(\tilde{\xi} - \tilde{\beta}a)$, which is equivalent to the condition

$$(a + \tilde{\beta})^2 < 4\tilde{\xi}. \tag{25}$$

To illustrate here the usefulness of our previous results, let us consider the focus-saddle bifurcation undergone by system (23)-(24) under condition (25) and hypotheses of Proposition 3 when $\tilde{h} = \tilde{a}$ for some specific choice of parameters. We remark that in such a case, we can neglect the left external zone $x < -1$, since for small values of $|\tilde{h} - \tilde{a}|$ the relevant dynamics involves only the adjacent zones to the boundary at $x = 1$. The first preparation task is to do the translation $X = x - 1$, $Y = y - a$, to get a continuous system in the form (3) with $a_{11}^L = -a$, $a_{11}^R = -b$, $a_{12} = 1$, $a_{21}^L = a_{21}^R = -\tilde{\xi}$, $a_{22}^L = a_{22}^R = \tilde{\beta}$, along with $b_1 = 0$, $b_2^L = b_2^R = \tilde{h} - \tilde{\xi} + \tilde{\beta}a = \tilde{h} - \tilde{a}$. Now a change of variables as the one used to obtain system (4) (which turns out to be homogeneous in this case, since $b_1 = 0$) transforms our system in a continuous version of such family, with $t_L = \tilde{\beta} - a$, $t_R = \tilde{\beta} - b$, $d_L = \tilde{\xi} - a\tilde{\beta}$, $d_R = \tilde{\xi} - b\tilde{\beta}$, and the bifurcation parameter is $\mu = \mu_L = \mu_R = \tilde{h} - \tilde{a}$.

Let us assume, following [15], the values $\alpha = 1.25$, $\beta = \xi = 1$, $a = 0.75$ and $b = 1.5$. Note that the specific passivity condition $0 < a < b$ is fulfilled. Thus, we get $\tilde{\beta} = \tilde{\xi} = 0.8$, $d_L = \tilde{a} = 0.2$ and $d_R = \tilde{b} = -0.4$, so that $t_L = 0.05$ and $t_R = -0.7$. Apart from the necessary condition for oscillating behaviour $a < \tilde{\beta} < b$, we see that both the external saddle dynamics condition $a\tilde{\beta} < \tilde{\xi} < b\tilde{\beta}$ and the focus condition (25) hold. Next, we apply Theorem 2.

Using (6) and (11), we get $\omega_L \approx 0.446514$, $\gamma_L \approx 0.055989$, $\omega_R \approx 0.722842$, $\gamma_R \approx -0.4842$, and $\rho \approx 0.809427$. Now from (8) we obtain $\theta_+ \approx 1.12858$ and $\theta_- \approx -0.717745$. Finally, from (12) we deduce $\delta \approx -0.140354 < 0$, and then statement (a) of Theorem 2 assures that for $\mu < 0$, that is, for $\tilde{h} < \tilde{a}$ there appears one stable limit cycle surrounding the unstable focus. This limit cycle (responsible for the stable oscillation in the circuit) grows linearly with $|\tilde{h} - \tilde{a}|$ as long as the assumption regarding that the cycle does not use the zone $x < -1$ is true. In fact, we could show the existence of a certain value $\tilde{h}_T > 0$, such that the limit cycle becomes tangent to the line $x = -1$. Thus, the existence of stable oscillations is guaranteed for all $\tilde{h}_T < \tilde{h} < \tilde{a}$. Furthermore, the symmetry of the model allows us to assure also the existence of stable oscillations for $-\tilde{a} < \tilde{h} < -\tilde{h}_T$. We conjecture that such oscillations exist indeed for all $-\tilde{a} < \tilde{h} < \tilde{a}$, but the proof of this conjecture is beyond the scope of this paper.

If we take instead $a = 0.74$, keeping fixed the rest of parameters, we have now $t_L = 0.06$, $d_L = \tilde{a} = 0.208$, $\omega_L \approx 0.455082$, $\gamma_L \approx 0.0659221$, and then we get $\rho \approx 0.825955$, $\theta_+ \approx 1.11361$ and $\theta_- \approx -0.711476$. However, now $\delta \approx 0.0363403 > 0$ and so the bifurcation does not lead to any limit cycle. Numerically, one can estimate that the critical value for the appearance of

the homoclinic orbit in the bifurcation is $a \approx 0.742014$.

3. Auxiliary results and proofs

In order to show the results of Section 1, it is convenient to reduce even more the number of essential parameters by rescaling time in a different way on each half-plane along with an appropriate rescaling of variables to maintain the canonical form. Note that this change of variables preserves any closed orbits. Afterwards, we obtain a useful reduced canonical form for the study of the focus-saddle configuration in refracting systems.

Proposition 4 *If $4d_L - t_L^2 > 0$ and $d_R < 0$ then refracting systems (4) can be written in the following reduced canonical form*

$$\begin{aligned} \frac{d\mathbf{x}}{d\theta_L} &= \begin{pmatrix} 2\gamma_L & -1 \\ \gamma_L^2 + 1 & 0 \end{pmatrix} \mathbf{x} - \begin{pmatrix} 0 \\ \alpha_L \end{pmatrix} \quad \textit{if } \mathbf{x} \in S_L \cup \Sigma, \\ \frac{d\mathbf{x}}{d\theta_R} &= \begin{pmatrix} 2\gamma_R & -1 \\ \gamma_R^2 - 1 & 0 \end{pmatrix} \mathbf{x} - \begin{pmatrix} 0 \\ \alpha_R \end{pmatrix} \quad \textit{if } \mathbf{x} \in S_R, \end{aligned} \tag{26}$$

where

$$\omega_L = \frac{\sqrt{4d_L - t_L^2}}{2}, \quad \gamma_L = \frac{t_L}{2\omega_L}, \quad \alpha_L = \frac{\mu_L}{\omega_L}, \tag{27}$$

and

$$\omega_R = \frac{\sqrt{t_R^2 - 4d_R}}{2}, \quad \gamma_R = \frac{t_R}{2\omega_R} \in (-1, 1), \quad \alpha_R = \frac{\mu_R}{\omega_R}. \tag{28}$$

Proof. We know that the eigenvalues of the linear part at S_L in (4) are $\sigma_L \pm i\omega_L$. We make first the change $X = \omega_L x$, $Y = y$, $\theta_L = \omega_L s$ for the

variables in the half plane S_L, without altering variables and time in S_R. Note that we do not change the coordinate y, so that periodic orbits using both half planes are preserved. Then, we get

$$\begin{aligned}\frac{dX}{d\theta_L} &= \frac{1}{\omega_L}\frac{dX}{ds} = \frac{dx}{ds} = \frac{t_L}{\omega_L}X - Y,\\ \frac{dY}{d\theta_L} &= \frac{1}{\omega_L}\frac{dY}{ds} = \frac{1}{\omega_L}\frac{dy}{ds} = \frac{1}{\omega_L}\left(\frac{d_L}{\omega_L}X - \mu_L\right) = \frac{d_L}{\omega_L^2}X - \frac{\mu_L}{\omega_L}.\end{aligned}$$

Introducing the parameter γ_L defined in (27), we see that $t_L = 2\gamma_L\omega_L$ and $d_L = (\gamma_L^2+1)\omega_L^2$, and the left vector field is already in form of (26).

Similarly to what is done in the left zone, we define $\omega_R > 0$ such that $\omega_R^2 = t_R^2/4 - d_R$ and $\sigma_R = t_R/2$, that is, the eigenvalues of the linear part at S_R in (4) are $\sigma_R \pm \omega_R$. In the same way as before, we make the change $X = \omega_R x$, $Y = y$, $\theta_R = \omega_R s$ for the variables in the half plane S_R, without altering variables and time in S_L. We obtain

$$\begin{aligned}\frac{dX}{d\theta_R} &= \frac{1}{\omega_R}\frac{dX}{ds} = \frac{dx}{ds} = \frac{t_R}{\omega_R}X - Y,\\ \frac{dY}{d\theta_R} &= \frac{1}{\omega_R}\frac{dY}{ds} = \frac{1}{\omega_R}\frac{dy}{ds} = \frac{1}{\omega_R}\left(\frac{d_R}{\omega_R}X - \mu_R\right) = \frac{d_R}{\omega_R^2}X - \frac{\mu_R}{\omega_R}.\end{aligned}$$

Now, introducing the parameter γ_R as in (28), we see that $t_R = 2\gamma_R\omega_R$ and $d_R = (\gamma_R^2-1)\omega_R^2$. Finally, using the definitions of α_L and α_R in (27)-(28), we get the expressions given in (26).

Note that under hypotheses of Proposition 4, if we assume $t_L > 0$ and $t_R < 0$ then we have $\gamma_L > 0$ and $-1 < \gamma_R < 0$. In the canonical form (26),

under hypotheses $\alpha_L < 0$, $\alpha_R < 0$, we have a focus at the point

$$\left(x^F, y^F\right) = \left(\frac{\alpha_L}{\gamma_L^2 + 1}, \frac{2\alpha_L\gamma_L}{\gamma_L^2 + 1}\right) \in S_L,$$

and a saddle at

$$\left(x^S, y^S\right) = \left(\frac{\alpha_R}{\gamma_R^2 - 1}, \frac{2\alpha_R\gamma_R}{\gamma_R^2 - 1}\right) \in S_R.$$

We can compute the points $(0, \tilde{y}_\pm)$ where the unstable (stable) manifold of the saddle intersects Σ as follows. The eigenvectors for the saddle can be selected as $(1, \gamma_R \mp 1)^T$ corresponding to the eigenvalues $\gamma_R \pm 1$. Thus, the linear invariant manifolds that emanate from the saddle intersect Σ when, for a certain value of β, we have

$$\begin{pmatrix} x^S \\ y^S \end{pmatrix} + \beta \begin{pmatrix} 1 \\ \gamma_R \mp 1 \end{pmatrix} = \begin{pmatrix} 0 \\ \tilde{y}_\pm \end{pmatrix}.$$

Clearly, $\beta = -x^S$ and then we get

$$\tilde{y}_\pm = \frac{2\alpha_R\gamma_R}{\gamma_R^2 - 1} - \frac{\alpha_R(\gamma_R \mp 1)}{\gamma_R^2 - 1} = \frac{\alpha_R(\gamma_R \pm 1)}{\gamma_R^2 - 1} = \frac{\alpha_R}{\gamma_R \mp 1}.$$

In the next result, we review some useful properties of the half-return maps that can be defined by using Σ as a Poincaré section, see Fig. 4. Generically, these half-return maps cannot be explicitly computed and must be obtained in parametric form in terms of the respective *flight times* θ_L and θ_R. Their properties can be straightforward deduced from the solutions of the linear vector field involved, see Proposition 6 and 7 of [19] and Proposition 3 of [20].

Proposition 5 *Considering systems* (26) *with* $\gamma_L > 0$, $-1 < \gamma_R < 0$, $\alpha_L < 0$ *and* $\alpha_R < 0$, *the following statements hold.*

a) The right Poincaré half-return map P_R *is defined only for* $\tilde{y}_- < y < 0$, *and is always bounded, so that* $0 \leq P_R(y) < \tilde{y}_+$. *Its parametric expressions are*

$$y = \alpha_R \frac{e^{-\gamma_R \theta_R} - \cosh\theta_R + \gamma_R \sinh\theta_R}{(\gamma_R^2 - 1)\sinh\theta_R},$$

$$P_R(y) = -\alpha_R \frac{e^{\gamma_R \theta_R} - \cosh\theta_R - \gamma_R \sinh\theta_R}{(\gamma_R^2 - 1)\sinh\theta_R},$$

where $\theta_R \in (0, \infty)$. *The first derivative satisfies* $\lim_{y \to \tilde{y}_-} P_R'(y) = 0$, *and the second derivative satisfies* $P_R''(y) < 0$ *for all* $y < 0$. *The function can be analytically extended to the origin by writing* $P_R(0) = 0$ *and then* $P_R'(0) = -1$.

b) Introducing the auxiliary function $\varphi_\gamma(\theta) = 1 - e^{\gamma\theta}(\cos\theta - \gamma \sin\theta)$, *the left Poincaré half-return map* P_L *is defined for all* $y \geq 0$, *and their parametric expressions are*

$$y = \alpha_L \frac{e^{-\gamma_L \theta_L} \varphi_{\gamma_L}(\theta_L)}{(\gamma_L^2 + 1)\sin\theta_L}, \quad P_L(y) = -\alpha_L \frac{e^{\gamma_L \theta_L} \varphi_{-\gamma_L}(\theta_L)}{(\gamma_L^2 + 1)\sin\theta_L}, \tag{29}$$

where $\theta_L \in (\pi, \hat{\theta})$, *being* $\hat{\theta}$ *the unique zero in* $(\pi, 2\pi)$ *of* φ_{γ_L}, *that is,* $\varphi_{\gamma_L}(\hat{\theta}) = 0$.

Furthermore, using that $y(\hat{\theta}) = 0$ *in* (29), *the image of the origin under the map is the point* $(0, \hat{y})$ *with* $\hat{y} = P_L(0) = -\alpha_L e^{\gamma_L \hat{\theta}} \sin\hat{\theta} < 0$ *(after*

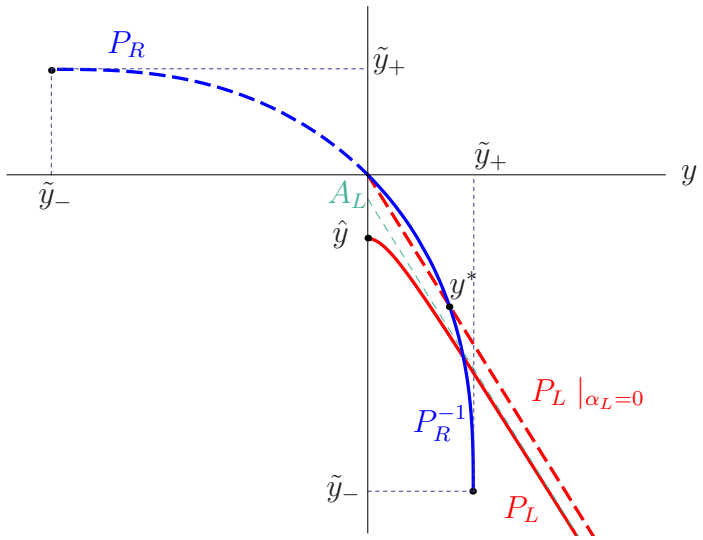

Figure 4: The graphs of the half-return Poincaré maps when $\gamma_L > 0$, $-1 < \gamma_R < 0$, $\alpha_L \leq 0$, $\alpha_R < 0$. The asymptote A_L for P_L when $\alpha_L < 0$ is parallel to the graph of P_L when $\alpha_L = 0$.

simplification), and we have

$$P_L : [0, \infty) \longrightarrow (-\infty, \hat{y}].$$

Moreover, $\lim_{y \to 0^+} P_L'(y) = 0$, $\lim_{y \to \infty} P_L'(y) = -e^{\pi\gamma_L}$, $P_L''(y) < 0$ *for all* $y > 0$, *and the graph of* P_L *has the asymptote*

$$A_L(y) = -e^{\pi\gamma_L} y + \frac{2\alpha_L\gamma_L}{\gamma_L^2 + 1}\left(1 + e^{\pi\gamma_L}\right).$$

Remark 5. The parametric expressions in terms of the flight time θ_L of Proposition 5-(b) are no longer valid when the focus is located at Σ, since then the left return time is equal to π for all the points in the domain. However, this exceptional case, corresponding to $\alpha_L = 0$, can be easily managed.

Effectively, a simple computation shows that then $P_L(y) = -e^{\pi\gamma_L} y$, for all $y > 0$, and so its graph is a straight line (the thick, dashed one in Figure 4).

Next, to show the uniqueness of closed orbits in systems (26), we use the non-generic case $\alpha_L = 0$, when the focus is located at the boundary, as a reference case for the more general situation $\alpha_L < 0$.

Proposition 6 *Considering refracting systems* (26) *with* $\gamma_L > 0$, $-1 < \gamma_R < 0$, $\alpha_L = 0$, $\alpha_R < 0$, *the following statements hold.*

a) If $e^{\pi\gamma_L} < (1-\gamma_R)/(1+\gamma_R)$, *then there exists one stable limit cycle surrounding the unstable boundary focus at the origin and there are no homoclinic connections.*

b) If $e^{\pi\gamma_L} = (1-\gamma_R)/(1+\gamma_R)$, *then there exists one homoclinic connection to the saddle and there are no periodic orbits surrounding the boundary focus.*

c) If $e^{\pi\gamma_L} > (1-\gamma_R)/(1+\gamma_R)$, *then the system has no periodic orbits and no homoclinic connections.*

Proof. Under our hypotheses, using Remark 5, we know that $P_L(y) = -e^{\pi\gamma_L} y$. Clearly, the limit cycles of the system are in one-to-one correspondence with the intersection points of the graphs of P_L and P_R^{-1}, see for instance [10] and Fig. 4.

From Proposition 5, using the concavity of the graph of P_R, the maximum number of intersections is one, and there is one intersection if and only if

$$-e^{\pi\gamma_L} \geq \frac{\tilde{y}_-}{\tilde{y}_+} = \frac{\gamma_R - 1}{\gamma_R + 1}.$$

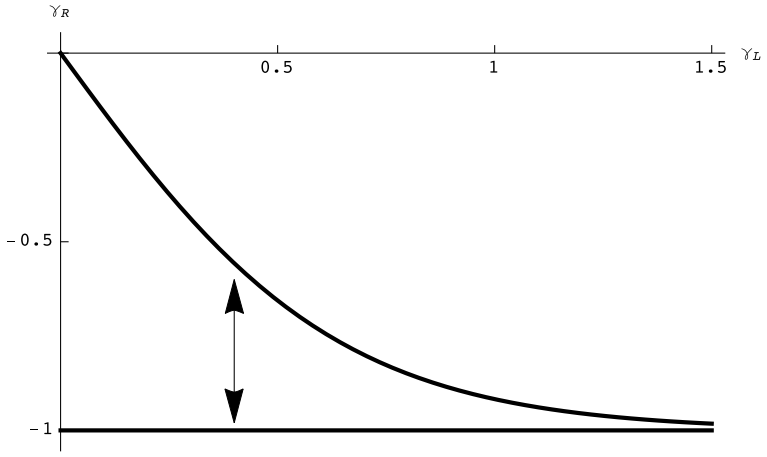

Figure 5: The open region in the plane (γ_L, γ_R) where it is possible the existence of a limit cycle or a homoclinic connection for systems (26) with $\gamma_L > 0$, $-1 < \gamma_R < 0$, $\alpha_L < 0$ and $\alpha_R < 0$, according to necessary condition (30).

From this condition, all the statements follow, if we take into account that the equality above leads to the existence of a homoclinic connection.

After changing the hypothesis $\alpha_L = 0$ to $\alpha_L < 0$, a simple necessary condition can be obtained.

Corollary 1 *Considering refracting systems* (26) *with* $\gamma_L > 0$, $-1 < \gamma_R < 0$, $\alpha_L < 0$ *and* $\alpha_R < 0$, *a necessary condition for the existence of a limit cycle or a homoclinic connection is*

$$e^{\pi\gamma_L} < \frac{1-\gamma_R}{1+\gamma_R}, \quad \textit{or equivalently,} \quad \gamma_R < -\tanh\left(\frac{\pi\gamma_L}{2}\right) \tag{30}$$

Corollary 1 follows from the fact that when $\alpha_L < 0$, the graph of P_L is below the graph of the asymptote A_L, which is in turn a straight-line parallel from below to the graph of $P_L\,|_{\alpha_L=0}$, see Fig. 4.

In figure 5, it is shown in the plane (γ_L, γ_R) the open region where the necessary condition (30) is fulfilled. Next, under same hypotheses of the above corollary, we give the proof of the uniqueness result of Proposition 2, which is more involved.

Proof of Proposition 2. We start by applying Proposition 4 to get the corresponding system (26) with $\alpha_L < 0$ and $\alpha_R < 0$. Recall that when $\alpha_L < 0$ the concavity for the graph of P_L is the same than for P_R. We will denote by $(y^*, -e^{\pi\gamma_L} y^*)$ the point of intersection of the graph of P_R^{-1} with the parallel to the asymptote A_L passing through the origin, that is, with the graph of P_L if we had taken all the parameters equal but $\alpha_L = 0$, see Fig. 4. Note that at such a point we must have

$$\left(P_R^{-1}\right)'(y^*) < -e^{\pi\gamma_L}. \tag{31}$$

Clearly, from Proposition 5, if there is any intersection between the two graphs, then it should be in a point with $y > y^*$. Suppose that there are two intersections points corresponding to $y = y_1$ and $y = y_2$, where $y^* < y_1 < y_2 \leq \tilde{y}_+$. In other words, we are assuming that

$$P_L(y_1) = P_R^{-1}(y_1), \quad P_L(y_2) = P_R^{-1}(y_2).$$

Then by Rolle's theorem there should be some intermediate point y where

$$P_L'(y) = \left(P_R^{-1}\right)'(y)$$

but we claim that this is impossible. Effectively, we know that

$$0 > P_L'(y) > -e^{\pi\gamma_L}$$

for all $y > 0$, and on the other hand, recalling (31)

$$\left(P_R^{-1}\right)'(y) < \left(P_R^{-1}\right)'(y^*) < -e^{-\pi\gamma_L},$$

getting the required contradiction. Note that the stability of the limit cycle (and for the homoclinic connection, as seen from its interior) comes easily by using that

$$P_L'(y) - \left(P_R^{-1}\right)'(y) > 0$$

in any intersection of both graphs.

It follows the proof of Theorem 1.

Proof of Theorem 1. We start again by applying Proposition 4 to get the corresponding system (26) with $\alpha_L < 0$ and $\alpha_R < 0$. For convenience, we make next the global translation $x \to x + x^F$, $y \to y + y^F$, to put the focus at the origin. To alleviate notation, we define the positive constant

$$v = -x^F = -\frac{\alpha_L}{\gamma_L^2 + 1} > 0, \tag{32}$$

so that $(x^F, y^F) = (-v, -2v\gamma_L)$. Thus, we work with the equivalent system

$$\begin{aligned}
\dot{\mathbf{x}} &= \begin{pmatrix} 2\gamma_L & -1 \\ \gamma_L^2 + 1 & 0 \end{pmatrix} \mathbf{x}, \text{ if } \mathbf{x} \in \widetilde{S}_L \cup \widetilde{\Sigma}, \\
\dot{\mathbf{x}} &= \begin{pmatrix} 2\gamma_R & -1 \\ \gamma_R^2 - 1 & 0 \end{pmatrix} \mathbf{x} - \begin{pmatrix} 2v(\gamma_R - \gamma_L) \\ \alpha_R + v\,(\gamma_R^2 - 1) \end{pmatrix}, \text{ if } \mathbf{x} \in \widetilde{S}_R,
\end{aligned} \tag{33}$$

where the linearity regions in the phase plane are now the left and right half-planes

$$\widetilde{S}_L = \{(x, y) \in \mathbb{R}^2 : x < v\}, \quad \widetilde{S}_R = \{(x, y) \in \mathbb{R}^2 : x > v\},$$

separated by the straight line $\widetilde{\Sigma} = \{(x, y) \in \mathbb{R}^2 : x = v\}$. Furthermore, the saddle point becomes the point

$$(\tilde{x}^S, \tilde{y}^S) = \left(v + \frac{\alpha_R}{\gamma_R^2 - 1}, 2v\gamma_L + \frac{2\alpha_R\gamma_R}{\gamma_R^2 - 1} \right),$$

which after introducing the positive parameter

$$\rho = \frac{\alpha_R}{\alpha_L} \cdot \frac{1 + \gamma_L^2}{1 - \gamma_R^2} = \frac{\mu_R}{\mu_L} \cdot \frac{\omega_L(1 + \gamma_L^2)}{\omega_R(1 - \gamma_R^2)} > 0, \tag{34}$$

can be written in the more compact expression

$$(\tilde{x}^S, \tilde{y}^S) = v\,(1 + \rho, 2(\gamma_L + \rho\gamma_R)), \tag{35}$$

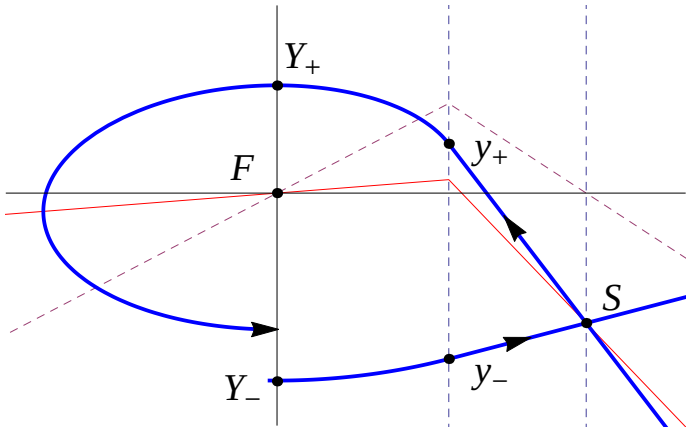

Figure 6: Sketch of the process to determine the remarkable points $(0, Y_\pm)$. The focus F is already put at the origin, so that the dashed vertical lines are the discontinuity manifold $\widetilde{\Sigma}$ at $x = v$, and the line $x = v + x_R^S$, where the saddle S is located.

since from (32) we have

$$\frac{\alpha_R}{\gamma_R^2 - 1} = v\rho.$$

The linear invariant manifolds that emanate from the saddle intersect the line $x = v$ at the points $(v, y_\pm)$ when, for a certain value of β, we have

$$\begin{pmatrix} \tilde{x}^S \\ \tilde{y}^S \end{pmatrix} + \beta \begin{pmatrix} 1 \\ \gamma_R \mp 1 \end{pmatrix} = \begin{pmatrix} v \\ y_\pm \end{pmatrix}.$$

Taking into account (35), we get $\beta = v - \tilde{x}^S = v - v(1 + \rho) = -v\rho$, and so the invariant manifolds of the saddle intersect the line $x = v$ at the points $(v, y_\pm)$, where

$$y_\pm = v\left[2\gamma_L + \rho(\gamma_R \pm 1)\right], \tag{36}$$

see Fig. 6.

We will follow the orbit with initial point (v, y_+) up to determine its

intersection point $(0, Y_+)$ with the new y-axis. Similarly, we can compute the point $(0, Y_-)$ whose orbit eventually arrives at the point (v, y_-) by integrating backwards in time from this latter point. Since the focus is at the origin, taking $(v, y_\pm)$ as the starting point, to compute now the value of $Y_\pm$, it suffices to write the exponential matrix and to solve the equation

$$\begin{pmatrix} 0 \\ Y_\pm \end{pmatrix} = e^{\gamma_L \theta_\pm} \begin{pmatrix} \cos\theta_\pm + \gamma_L \sin\theta_\pm & -\sin\theta_\pm \\ (\gamma_L^2+1)\sin\theta_\pm & \cos\theta_\pm - \gamma_L \sin\theta_\pm \end{pmatrix} \begin{pmatrix} v \\ y_\pm \end{pmatrix}, \tag{37}$$

where the flight times must satisfy $0 < \pm\theta_\pm < \pi$, since we must integrate forward (backward) in time to get Y_+ (Y_-), see Fig. 6.

From the first component of equality in (37), we get

$$v\cos\theta_\pm = (y_+ - v\gamma_L)\sin\theta_\pm = v\left[\gamma_L + \rho(\gamma_R \pm 1)\right]\sin\theta_\pm. \tag{38}$$

Equivalently, we write

$$\tan\theta_\pm = \frac{1}{\gamma_L + \rho(\gamma_R \pm 1)},$$

and we obtain

$$\sin\theta_\pm = \pm\frac{|\tan\theta_\pm|}{\sqrt{1+\tan^2\theta_\pm}} = \pm\frac{1}{\sqrt{1+\left[\gamma_L + \rho(\gamma_R \pm 1)\right]^2}},$$

and then

$$\cos\theta_\pm = \pm\frac{\gamma_L + \rho(\gamma_R \pm 1)}{\sqrt{1+\left[\gamma_L + \rho(\gamma_R \pm 1)\right]^2}}.$$

To ease the angle determination with the arctan function, we use the

trigonometric identity

$$\tan\left(\frac{\theta_\pm}{2}\right) = \frac{\sin\theta_\pm}{1+\cos\theta_\pm} = \pm\frac{1}{\sqrt{1+\left[\gamma_L+\rho(\gamma_R\pm 1)\right]^2}\pm\left[\gamma_L+\rho(\gamma_R\pm 1)\right]}.$$

After multiplying numerator and denominator in the argument by the conjugate, we get

$$\theta_\pm = \pm 2\arctan\left(\sqrt{1+\left[\gamma_L+\rho(\gamma_R\pm 1)\right]^2}\mp\left[\gamma_L+\rho(\gamma_R\pm 1)\right]\right), \qquad (39)$$

as given in (8). Noting that $\cos\theta_\pm - \gamma_L\sin\theta_\pm = \rho(\gamma_R\pm 1)\sin\theta_\pm$, we get from the second component of equality of (37) that

$$Y_\pm = e^{\gamma_L\theta_\pm}\left[(\gamma_L^2+1)v+\rho(\gamma_R\pm 1)y_\pm\right]\sin\theta_\pm = \pm v e^{\gamma_L\theta_\pm}\sqrt{1+\left[\gamma_L+\rho(\gamma_R\pm 1)\right]^2},$$

where $\theta_\pm$ is given in (39) and we have used the above expresions for $y_\pm$ and $\sin\theta_\pm$, leading to

$$(\gamma_L^2+1)v+\rho(\gamma_R\pm 1)y_\pm = v\left(1+\left[\gamma_L+\rho(\gamma_R\pm 1)\right]^2\right).$$

Therefore, the common expression for both ordinates is $Y_\pm = vV_\pm$, with $V_\pm$ as given in (9).

Summarizing, the unstable invariant manifold of the saddle after intersecting the vertical $x = v$ at the point (v, y_+) passes through the point $(0, Y_+)$ and will come back again to the new y-axis at the point $(0, -e^{\pi\gamma_L}Y_+)$. Analogously, the linear stable invariant manifold of the saddle is reached when we consider the orbit starting at the point $(0, Y_-)$, see Fig. 6.

Assume first that $-e^{\pi\gamma_L}Y_+ > Y_-$, which after reordering and removing the common factor v leads to $e^{\pi\gamma_L}V_+ + V_- < 0$. Then we have a trapping region containing the unstable focus, so that by Poincaré-Bendixson's theorem we must have at least a periodic orbit surrounding the focus. The uniqueness and stability of the corresponding limit cycle comes from Proposition 2 and statement (a) follows.

To show statement (b) it suffices to see that if the condition of the statement holds, then the two linear invariant manifolds of the saddle are connected forming a saddle-loop or homoclinic connection. Therefore, from Proposition 2 there cannot be limit cycles.

In the case of statement (c), since $-e^{\pi\gamma_L}Y_+ < Y_-$, we conclude that for the original system (26) we have $P_L(\tilde{y}_+) < \tilde{y}_-$, see Fig. 4. Then, regarding the proof of Proposition 2, if there exists an intersection between the graphs of P_L and P_R^{-1}, then the concavity of both graphs implies the existence of at least two intersection points below the point y^*. This is impossible, as shown in Proposition 2, so that we conclude that there are no limit cycles. The theorem is so completely shown.

Finally, we give the proof of Theorem 2.

Proof of Theorem 2. All the assertions about the equilibrium points and their stability come easily from Proposition 1, taking into account the hypothesis $4d_L - t_L^2 > 0$.

Applying Proposition 4, we arrive at a system (26) with $\alpha_L = \mu/\omega_L$, $\alpha_R = \mu/\omega_R$. Note that even we start from a continuous vector field in (4), after the transformation involved in the quoted proposition, we pass to a

refracting system. This is the reason why we needed to consider the more general framework of discontinuous refracting systems.

Note also that from (34) the parameter ρ becomes

$$\rho = \frac{\omega_L(1+\gamma_L^2)}{\omega_R(1-\gamma_R^2)} > 0,$$

as given in (11), not depending on μ.

If μ is negative, then the appearance of a limit cycle, an homoclinic connection or nothing else, is a direct consequence of Theorem 1, considering the sign of the expression $e^{\pi\gamma_L}V_+ + V_-$. Taking into account that $e^{\pi\gamma_L}V_+ - V_- > 0$, we can write

$$\operatorname{sign}(e^{\pi\gamma_L}V_+ + V_-) = \operatorname{sign}(e^{2\pi\gamma_L}V_+^2 - V_-^2) = \operatorname{sign}\left(e^{2\gamma_L\pi} - \frac{V_-^2}{V_+^2}\right),$$

from where the expression of the coefficient δ follows.

To complete the proof, we need to show the linear evolution of the limit cycle or the saddle-loop with respect to $|\mu|$. It suffices to note that in systems (10), when $\mu \neq 0$, the system can be rewritten with $\mu = \pm 1$ by the homothety change $X = |\mu|x$, $Y = |\mu|y$. Therefore, if $\mu < 0$ and there exists a periodic orbit or an homoclinic connection, then there exists also the same distinguished closed orbit for $\mu = -1$ and both orbits are homothetic. So, the size of the such orbit evolves linearity with $|\mu|$, and the theorem follows.

Acknowledgements

Authors are partially supported by the *Spanish Ministerio de Economía, Industria y Competitividad*, in the frame of projects MTM2014-56272-C2-1-P

and MTM2015-65608-P, and by the *Consejería de Economía y Conocimiento* de la Junta de Andalucía under grant P12-FQM-1658.

References

[1] M. Di Bernardo, C. Budd, A. R. Champneys, P. Kowalczyk, Piecewise-smooth dynamical systems: theory and applications, Vol. 163 of Appl. Math. Sci., Springer-Verlag, 2007.

[2] D. Simpson, Bifurcations in Piecewise-Smooth Continuous Systems, World Scientific series on nonlinear science: A, World Scientific Publishing Company, Incorporated, 2010.

[3] M. Di Bernardo, D. Pagano, E. Ponce, Nonhyperbolic boundary equilibrium bifurcations in planar Filippov systems: a case study approach., International Journal of Bifurcation and Chaos in Applied Sciences and Engineering 18 (2008) 1377–1392.

[4] M. Guardia, T. Seara, M. Teixeira, Generic bifurcations of low codimension of planar Filippov systems, J. Differential Equations 250 (2011) 1967–2023.

[5] C. A. Buzzi, J. C. Medrado, M. A. Teixeira, Generic bifurcation of refracted systems, Advances in Mathematics 234 (2013) 653–666.

[6] Y. A. Kuznetsov, S. Rinaldi, A. Gragnani, One-parameter bifurcations in planar Filippov systems, I. J. Bifurcation and Chaos 13 (8) (2003) 2157–2188.

[7] J. C. Medrado, J. Torregrosa, Uniqueness of limit cycles for sewing planar piecewise linear systems, Journal of Mathematical Analysis and Applications 431 (1) (2015) 529–544. doi:10.1016/j.jmaa.2015.05.064.

[8] E. Freire, E. Ponce, F. Torres, Canonical discontinuous planar piecewise linear systems, SIAM Journal Applied Dynamical Systems 11 (2012) 181–211.

[9] J. Llibre, E. Ponce, F. Torres, On the existence and uniqueness of limit cycles in Liénard differential equations allowing discontinuities, Nonlinearity 21 (2008) 2121–2142.

[10] E. Ponce, J. Ros, E. Vela, Limit cycle and boundary equilibrium bifurcations in continuous planar piecewise linear systems, International Journal of Bifurcation and Chaos 25 (3) (2015) 1530008–01–1530008–18.

[11] J. Llibre, E. Ponce, C. Valls, Uniqueness and non-uniqueness of limit cycles for piecewise linear differential systems with three zones and no symmetry, J. Nonlinear Science 25 (2015) 861–887.

[12] E. Freire, E. Ponce, F. Rodrigo, F. Torres, Bifurcation sets of continuous piecewise linear systems with two zones, Int. J. Bifurcation and Chaos 8 (1998) 2073–2097.

[13] E. Ponce, J. Ros, E. Vela, Progress and Challenges in Dynamical Systems, Vol. 54 of Springer Proceedings in Mathematics & Statistics, Springer, 2013, Ch. The focus-center-limit cycle bifurcation in discontinuous planar piecewise linear systems without sliding, pp. 335–349.

[14] D. Simpson, J. Meiss, Andronov-Hopf bifurcations in planar, piecewise-smooth, continuous flows, Physics Letters A 371 (2007) 213– 220.

[15] F. Corinto, A. Ascoli, M. Gilli, Nonlinear dynamics of memristor oscillators, IEEE Trans. Circuits and Systems I: Regular papers 58 (2011) 1323–1336.

[16] F. Corinto, M. Forti, Memristor circuits: Flux-charge analysis method, IEEE Trans. Circuits and Systems I: Regular papers 63 (2016) 1997–2009.

[17] L. O. Chua, Memristor: The missing circuit element, IEEE Trans. Circuit Theory CT-18 (1971) 507–519.

[18] M. Itoh, L. Chua, Memristor oscillators, Int. J. Bifurcation and Chaos 18 (2008) 3183–3206.

[19] E. Freire, E. Ponce, F. Torres, A general mechanism to generate three limit cycles in planar Filippov systems with two zones, Nonlinear Dynamics 78 (2014) 251–263.

[20] E. Freire, E. Ponce, F. Torres, The discontinuous matching of two planar foci can have three nested crossing limit cycles, Publicacions Matemàtiques Extra (2014) 221–253.